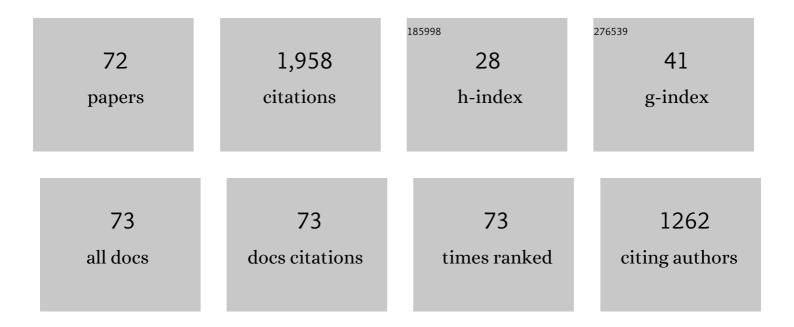
Thilo F Morgeneyer

List of Publications by Year in descending order

Source: https://exaly.com/author-pdf/2528204/publications.pdf Version: 2024-02-01



#	Article	IF	CITATIONS
1	In situ 3-D observation of early strain localization during failure of thin Al alloy (2198) sheet. Acta Materialia, 2014, 69, 78-91.	3.8	100
2	Quench sensitivity of toughness in an Al alloy: Direct observation and analysis of failure initiation at the precipitate-free zone. Acta Materialia, 2008, 56, 2872-2884.	3.8	86
3	Evolution of voids during ductile crack propagation in an aluminium alloy sheet toughness test studied by synchrotron radiation computed tomography. Acta Materialia, 2008, 56, 1671-1679.	3.8	71
4	Real-time image-content-based beamline control for smart 4D X-ray imaging. Journal of Synchrotron Radiation, 2016, 23, 1254-1263.	1.0	69
5	3D Digital Volume Correlation of Synchrotron Radiation Laminography Images of Ductile Crack Initiation: An Initial Feasibility Study. Experimental Mechanics, 2013, 53, 543-556.	1.1	66
6	Three-dimensional quantitative in situ study of crack initiation and propagation in AA6061 aluminum alloy sheets via synchrotron laminography and finite-element simulations. Acta Materialia, 2013, 61, 2571-2582.	3.8	66
7	Ductile damage mechanism under shear-dominated loading: In-situ tomography experiments on dual phase steel and localization analysis. International Journal of Plasticity, 2018, 109, 169-192.	4.1	64
8	Fatigue lifetime and tearing resistance of AA2198 Al–Cu–Li alloy friction stir welds: Effect of defects. International Journal of Fatigue, 2015, 70, 463-472.	2.8	59
9	Plastic flow and ductile rupture of a 2198 Al–Cu–Li aluminum alloy. Computational Materials Science, 2011, 50, 1365-1371.	1.4	55
10	Experimental and numerical analysis of toughness anisotropy in AA2139 Al-alloy sheet. Acta Materialia, 2009, 57, 3902-3915.	3.8	54
11	Damage of semicrystalline polyamide 6 assessed by 3D Xâ€ray tomography: From microstructural evolution to constitutive modeling. Journal of Polymer Science, Part B: Polymer Physics, 2010, 48, 1516-1525.	2.4	48
12	Ductile crack initiation and propagation assessed via in situ synchrotron radiation-computed laminography. Scripta Materialia, 2011, 65, 1010-1013.	2.6	47
13	Localized strain field measurement on laminography data with mechanical regularization. Nuclear Instruments & Methods in Physics Research B, 2014, 324, 70-79.	0.6	47
14	Effect of Multiaxial Stress State on Morphology and Spatial Distribution of Voids in Deformed Semicrystalline Polymer Assessed by X-ray Tomography. Macromolecules, 2012, 45, 4658-4668.	2.2	46
15	Flat to slant ductile fracture transition: Tomography examination and simulations using shear-controlled void nucleation. Scripta Materialia, 2011, 65, 1002-1005.	2.6	44
16	Intergranular damage during stress relaxation in AISI 316L-type austenitic stainless steels: Effect of carbon, nitrogen and phosphorus contents. Acta Materialia, 2016, 103, 893-908.	3.8	44
17	Numerical validation framework for micromechanical simulations based on synchrotron 3D imaging. Computational Mechanics, 2017, 59, 419-441.	2.2	43
18	Microstructural Characterization of Internal Welding Defects and Their Effect on the Tensile Behavior of FSW Joints of AA2198 Al-Cu-Li Alloy. Metallurgical and Materials Transactions A: Physical Metallurgy and Materials Science, 2014, 45, 5531-5544.	1.1	41

THILO F MORGENEYER

#	Article	IF	CITATIONS
19	In situ laminography study of three-dimensional individual void shape evolution at crack initiation and comparison with Gurson–Tvergaard–Needleman-type simulations. Acta Materialia, 2014, 78, 254-270.	3.8	41
20	Damage observation in a high-manganese austenitic TWIP steel by synchrotron radiation computed tomography. Scripta Materialia, 2010, 63, 1220-1223.	2.6	38
21	On the choice of boundary conditions for micromechanical simulations based on 3DÂimaging. International Journal of Solids and Structures, 2017, 112, 83-96.	1.3	37
22	Influence of strain rate on P92 microstructural stability during fatigue tests at high temperature. Procedia Engineering, 2010, 2, 2141-2150.	1.2	36
23	Nanovoid morphology and distribution in deformed HDPE studied by magnified synchrotron radiation holotomography. Polymer, 2014, 55, 6439-6443.	1.8	36
24	On the crystallographic, stage I-like, character of fine granular area formation in internal fish-eye fatigue cracks. International Journal of Fatigue, 2018, 106, 132-142.	2.8	36
25	Effect of joint line remnant on fatigue lifetime of friction stir welded Al–Cu–Li alloy. Science and Technology of Welding and Joining, 2010, 15, 694-698.	1.5	34
26	Three dimensional quantification of anisotropic void evolution in deformed semi-crystalline polyamide 6. International Journal of Plasticity, 2016, 83, 19-36.	4.1	34
27	On strain and damage interactions during tearing: 3D in situ measurements and simulations for a ductile alloy (AA2139-T3). Journal of the Mechanics and Physics of Solids, 2016, 96, 550-571.	2.3	32
28	Void growth and coalescence in a magnesium alloy studied by synchrotron radiation laminography. Acta Materialia, 2018, 155, 80-94.	3.8	31
29	Effect of hardening on toughness captured by stress-based damage nucleation in 6061 aluminum alloy. Acta Materialia, 2019, 180, 349-365.	3.8	29
30	Effect of void arrangement on ductile damage mechanisms in nodular graphite cast iron: In situ 3D measurements. Engineering Fracture Mechanics, 2018, 192, 242-261.	2.0	28
31	Synchrotron and neutron laminography for three-dimensional imaging of devices and flat material specimens. International Journal of Materials Research, 2012, 103, 170-173.	0.1	27
32	Ductile damage of AA2024-T3 under shear loading: Mechanism analysis through in-situ laminography. Acta Materialia, 2021, 205, 116556.	3.8	26
33	On the calibration of elastoplastic parameters at the microscale via X-ray microtomography and digital volume correlation for the simulation of ductile damage. European Journal of Mechanics, A/Solids, 2018, 72, 287-297.	2.1	24
34	Voiding Mechanisms in Deformed Polyamide 6 Observed at the Nanometric Scale. Macromolecules, 2017, 50, 4372-4383.	2.2	23
35	Three-dimensional investigation of thermal barrier coatings by synchrotron-radiation computed laminography. Scripta Materialia, 2012, 66, 471-474.	2.6	22
36	Slant strained band development during flat to slant crack transition in AA 2198 T8 sheet: in situ 3D measurements. International Journal of Fracture, 2016, 200, 49-62.	1.1	21

THILO F MORGENEYER

#	Article	IF	CITATIONS
37	On deformation and damage micromechanisms in strong work hardening 2198 T3 aluminium alloy. Acta Materialia, 2018, 149, 29-45.	3.8	20
38	Failure of Magnesium Sheets Under Monotonic Loading: 3D Examination of Fracture Mode and Mechanisms. International Journal of Fracture, 2013, 183, 105-112.	1.1	19
39	A constitutive model accounting for strain ageing effects on work-hardening. Application to a C–Mn steel. Comptes Rendus - Mecanique, 2017, 345, 908-921.	2.1	19
40	Strength and fatigue strength of a similar Tiâ€6Alâ€2Snâ€4Zrâ€2Moâ€0.1Si linear friction welded joint. Fatigue and Fracture of Engineering Materials and Structures, 2019, 42, 1100-1117.	1.7	18
41	Bulk evaluation of ductile damage development using high resolution tomography and laminography. Comptes Rendus Physique, 2012, 13, 328-336.	0.3	17
42	Comparison of voiding mechanisms in semi-crystalline polyamide 6 during tensile and creep tests. Polymer Testing, 2016, 49, 137-146.	2.3	17
43	In situ 3D Synchrotron Laminography Assessment of Edge Fracture in Dual-Phase Steels: Quantitative and Numerical Analysis. Experimental Mechanics, 2016, 56, 177-195.	1.1	17
44	Evaluation of measurement uncertainties of digital volume correlation applied to laminography data. Journal of Strain Analysis for Engineering Design, 2018, 53, 49-65.	1.0	17
45	3D in situ study of damage during a â€~shear to tension' load path change in an aluminium alloy. Acta Materialia, 2022, 231, 117842.	3.8	17
46	Structural versus microstructural evolution of semi-crystalline polymers during necking under tension: Influence of the skin-core effects, the relative humidity and the strain rate. Polymer Testing, 2016, 55, 297-309.	2.3	16
47	Interaction of the Portevin–LeÂChatelier phenomenon with ductile fracture of a thin aluminum CT specimen: experiments and simulations. International Journal of Fracture, 2017, 206, 95-122.	1.1	16
48	Three-Dimensional Damage Evolution Measurement in EB-PVD TBCs Using Synchrotron Laminography. Oxidation of Metals, 2013, 79, 313-323.	1.0	14
49	On crystallographic aspects of heterogeneous plastic flow during ductile tearing: 3D measurements and crystal plasticity simulations for AA7075-T651. International Journal of Plasticity, 2021, 144, 103028.	4.1	14
50	Three-dimensional characterization of fatigue-relevant intermetallic particles in high-strength aluminium alloys using synchrotron X-ray nanotomography. Philosophical Magazine, 2015, 95, 2731-2746.	0.7	13
51	3D Damage Micromechanisms in Polyamide 6 Ahead of a Severe Notch Studied by <i>In Situ</i> Synchrotron Laminography. Macromolecular Chemistry and Physics, 2016, 217, 701-715.	1.1	13
52	Portevin-Le Chatelier effect triggered by complex loading paths in an Al–Cu aluminium alloy. Philosophical Magazine, 2019, 99, 659-678.	0.7	13
53	On the effect of a thermal treatment on the tensile and fatigue properties of weak zones of similar Ti17 linear friction welded joints and parent material. Materials Characterization, 2020, 169, 110570.	1.9	13
54	A comparative study of image segmentation methods for micromechanical simulations of ductile damage. Computational Materials Science, 2019, 159, 43-65.	1.4	12

THILO F MORGENEYER

#	Article	IF	CITATIONS
55	Nanocavitation mechanisms in deformed High Density PolyEthylene (HDPE) using synchrotron radiation NanoTomography. Polymer, 2021, 229, 123959.	1.8	10
56	Microstructural observations supporting thermography measurements for short glass fibre thermoplastic composites under fatigue loading. Continuum Mechanics and Thermodynamics, 2020, 32, 451-469.	1.4	9
57	Strength, fatigue strength and toughness of dissimilar Ti17–Ti64 linear friction welded joints: Effect of soft surface contamination and depletion of α precipitates. Materials Science & Engineering A: Structural Materials: Properties, Microstructure and Processing, 2021, 799, 139989.	2.6	9
58	Experimental Analysis of Toughness in 6156 Al-Alloy Sheet for Aerospace Applications. Materials Science Forum, 2006, 519-521, 1023-1028.	0.3	8
59	Impact of machine stiffness on â€~â€~pop-in'' crack propagation instabilities. Engineering Fracture Mechanics, 2018, 202, 405-422.	2.0	8
60	Numerical investigation of dynamic strain ageing and slant ductile fracture in a notched specimen and comparison with synchrotron tomography 3D-DVC. Procedia Structural Integrity, 2016, 2, 3385-3392.	0.3	7
61	Local approach to stress relaxation cracking in a AISI 316L-type austenitic stainless steel: Tomography damage quantification and FE simulations. Engineering Fracture Mechanics, 2017, 183, 170-179.	2.0	5
62	On the Origin of the Anisotropic Damage of X100 Line Pipe Steel: Part l—In Situ Synchrotron Tomography Experiments. Integrating Materials and Manufacturing Innovation, 2019, 8, 570-596.	1.2	5
63	Recent advances in finite element modelling of ductile fracture at mesoscale. Procedia Manufacturing, 2018, 15, 39-45.	1.9	2
64	Damage based model to study the effect of notch introduction technique on the J -integral value of PolyOxyMethylene. Engineering Fracture Mechanics, 2015, 149, 214-229.	2.0	1
65	In Situ Observation of Strained Bands and Ductile Damage in Thin AA2139-T3 Alloy Sheets. Procedia IUTAM, 2017, 20, 66-72.	1.2	1
66	3D Stress Fields Versus Void Distributions Ahead Of a Notch Tip For Semi-crystalline Polymers. Procedia Structural Integrity, 2018, 13, 1751-1755.	0.3	1
67	Quantitative Anisotropic Damage Mechanism in a Forged Aluminum Alloy Studied by Synchrotron Tomography and Finite Element Simulations. Advances in Materials Science and Engineering, 2019, 2019, 1-12.	1.0	1
68	On the use of stereoâ€digital image correlation for the alignment of a fatigue testing machine in accordance with international standards: A feasibility study. Strain, 2021, 57, e12382.	1.4	1
69	Numerical modeling of ductile fracture at the microscale combined with X-ray laminography and digital volume correlation. AIP Conference Proceedings, 2017, , .	0.3	Ο
70	Experimental-Numerical Validation Framework for Micromechanical Simulations. Lecture Notes in Applied and Computational Mechanics, 2018, , 147-161.	2.0	0
71	Early Strain Localization in Strong Work Hardening Aluminum Alloy (2198 T3): 3D Laminography and DVC Measurement. Conference Proceedings of the Society for Experimental Mechanics, 2018, , 15-17.	0.3	0
72	Effects of neutron irradiation and post-irradiation annealing on pop-in crack propagation instabilities in 6061 aluminium alloy. Journal of Nuclear Materials, 2022, , 153909.	1.3	0